Diffusive CH4 fluxes from aquaculture ponds using floating chambers and thin boundary layer equations

Diffusive CH_4 fluxes from aquaculture ponds using floating chambers and thin boundary layer equations

Ping Yang[a,b,1], Jiafang Huang[a,b,1], Hong Yang[c,d,e,1], Josep Peñuelas[f,g], Derrick Y.F. Lai[h*], Dongqi Wang[i], Qitao Xiao[j], Jordi Sardans[f,g,], Yifei Zhang[a,b], Chuan Tong[a,b,***]**

[a]*Key Laboratory of Humid Subtropical Eco-geographical Process of Ministry of Education, Fujian Normal University, Fuzhou 350007, P.R. China*

[b]*School of Geographical Sciences, Fujian Normal University, Fuzhou 350007, P.R. China*

[c]*College of Environmental Science and Engineering, Fujian Normal University, Fuzhou 350007, P.R. China*

[d]*Collaborative Innovation Center of Atmospheric Environment and Equipment Technology, Jiangsu Key Laboratory of Atmospheric Environment Monitoring and Pollution Control (AEMPC), School of Environmental Science and Engineering, Nanjing University of Information Science and Technology, Nanjing 210044, China;*

[e]*Department of Geography and Environmental Science, University of Reading, Reading RG6 6AB, U.K.*

[f]*CSIC, Global Ecology Unit CREAF-CSIC-UAB, Bellaterra, Catalonia, Spain*

[g]*CREAF, Cderdanyola del Vallès, Catalonia, Spain*

[h]*Department of Geography and Resource Management, The Chinese University of Hong Kong, Shatin, New Territories, Hong Kong SAR, China*

[i]*School of Geographical Sciences, East China Normal University, Shanghai 200241, China*

[j]*Key Laboratory of Watershed Geographic Sciences, Nanjing Institute of Geography and Limnology, Chinese Academy of Sciences, Nanjing, 210008, China*

***Correspondence to:** Derrick Y.F. Lai

Email: dyflai@cuhk.edu.hk

***Correspondence to:** Jordi Sardans

Email: j.sardans@creaf.uab.cat

****Correspondence to:** Chuan Tong

Email: tongch@fjnu.edu.cn

[1]Ping Yang, Jiafang Huang, and Hong Yang contributed equally to this work.

HIGHLIGHTS

- Aquaculture ponds emit CH4.
- Large variations in diffusive CH4 fluxes are estimated by different thin boundary layer (TBL) models.
- Methane fluxes measured by chambers and match those estimated by only some TBL models.

A B S T R A C T

Static floating chambers (*FCs*) are the conventional method to measure CH4 fluxes across the water-air interface in ponds, while thin boundary layer (*TBL*) modelling is increasingly used to estimate CH4 fluxes. In this study, both *FCs* measurements and *TBL* models of gas transfer velocity were used to determine CH4 evasion from aquaculture ponds in southeastern China. The surface water CH4 concentrations ranged from 0.4 to 9.1 μmol L-1 with an average of 4.8 ± 0.8 μmol L-1. CH4 flux was always positive, indicating the ponds as a persistent CH4 source to air. Mean CH4 flux based on different *TBL* models showed large variations, ranging between 19 and 316 μmol m−2 h−1. Compared against the direct measurement *FCs*, three *TBL* models developed for the open sea, flowing estuarine system and lentic ecosystem (*TBL*W92a, *TBL*RC01, and *TBL*CL98, respectively) overestimated CH4 emission by 40–200%, while the wind tunnel-based *TBL* model (*TBL*LM86) underestimated CH4 emission. Two *TBL* models developed for lakes (*TBL*W92b and *TBL*CW03) gave estimates similar to *FCs*.

Keywords: Methane fluxes; Thin boundary layer models; Floating chambers; Water-air interface; Shallow aquaculture pond; Subtropical estuary

1. Introduction

Methane (CH4) emissions from inland and coastal aquatic systems are potentially significant sources of atmospheric CH4 (Bastviken et al., 2011; Musenze et al., 2014; Yang et al., 2011). CH4 release from open water surfaces can take place via diffusion and/or ebullition (bubbling) (Bastviken et al., 2004). Diffusive fluxes across the water-air interface are traditionally measured by using static floating chambers (FCs) or thin boundary layer (TBL) model. The FCs approach determines CH4 fluxes based on the change in CH4 concentrations in the chamber headspace over time. The TBL approach calculates the CH4 flux using a piston velocity and gas concentration in the water (Natchimuthu et al., 2017; Zhao et al., 2019). *TBL* modelling can be used to estimate CH4 emissions from aquatic environment at a large-scale (Zhao et al., 2015), while static FCs measurements are widely operated to quantify the small-scale spatial variation in CH4 fluxes over an area of < 1 m2 (Denmead, 2008; Xiao et al., 2016). Previous studies have used either one of the two approaches to quantify CH_4 fluxes from aquatic ecosystems (e.g., Musenze et al., 2014; Natchimuthu et al., 2016; Wang et al., 2017; Welti et al., 2017). However, integrated comparative studies of these two methods for determining CH4 emissions from aquatic ecosystems remain scarce (e.g., Duchemin et al., 1999; Matthews et al., 2003), particularly in small pond ecosystems.

Recent studies have shown that very small ponds (area <0.001 km2) are hotspots of CH4 emission (Holgerson, 2015; Holgerson and Raymond, 2016; Wik et al., 2016; Yuan et al., 2019). However, the accuracy of these estimates are largely constrained by the lack of rigorous quantifications of the area, number, and spatial distribution of small ponds globally (Jonsson et al., 2008; Zhao et al., 2019) and the large variations in flux measurement methods between different studies. In particular, the lack of consensus between existing gas flux measurement methods remains a major source for the uncertainty of

GHGs accounting. This lack of agreement might be related to the variation in developing environment between methods. For instance, the TBLLM86, TBLWan92a and TBLWan92b, TBLRC01, TBLCL98, and TBLCW03 models which were developed by Liss and Merlivatt (1986), Wanninkhof (1992), Raymond and Cole (2001), Cole and Caraco (1998), and Crusius and Wanninkhof (2003), respectively, are widely accepted wind-based models to estimate CH4 transfer velocities and fluxes. Among these TBL models, the TBLLM86, TBLWan92a, and TBLRC01 models were developed in wind tunnels, open sea, and flowing estuarine systems, respectively, while TBWan92b, TBLCL98 and TBLCW03 models were established in the lentic ecosystem (e.g., lake). It is still unclear to what level of certainty these different models can accurately calculate the gas transfer velocities in various aquatic ecosystems (Musenze et al., 2014). Thus, a simple, low-cost, and standardized technique is still required for the accurate estimation of CH4 fluxes at the regional and global scales.

Aquaculture ponds form an important component of the global network of small ponds (FAO, 2017), and the total surface area of freshwater and brackish aquaculture ponds is estimated to be around 110,000 km2 (Verdegem and Bosma, 2009). Despite the importance of aquaculture ponds for CH4 emission (Hu et al., 2016; Wu et al., 2018; Yang et al., 2015, 2019a; Yuan et al., 2019), CH4 flux data are disproportionately scarce, and the published results were predominantly determined by FCs, rather than TBL modelling (Hu et al., 2016; Wu et al., 2018; Yang et al., 2015, 2019a). Clearly, there is a paucity of researches on comparing CH4 fluxes obtained by using different approaches. In this study, FCs and six TBL models were applied in aquacultural ponds in Southeast China, and the CH4 fluxes were compared. The primary research aims are: (1) to evaluate the performances of different wind-based TBL models for the estimation of CH4 fluxes; (2) to compare the diffusive CH4 emissions from aquaculture ponds derived from the FCs measurements and TBL modellings; and (3) to identify the TBL model(s) which can be

applied to replace the FCs for the measurement of CH4 fluxes from ponds, with the minimal uncertainty.

2. Materials and Methods

2.1. Study area

Our study sites were located at the central-western Shanyutan Wetlands in the Min River Estuary (MRE) in Southeast China (Figure S1, 26°00′36″–26°03′42″ N, 119°34′12″–119°40′40″ E). This area is characterized by a subtropical monsoon climate, with a multi-year average annual temperature and precipitation of 19.6 °C and 1,350 mm, respectively (Tong et al., 2010). The wetlands are dominated by a semidiurnal tide with a large tidal range (2.5-6 m) that follows a spring-neap-spring tidal cycle (Luo et al., 2014; Tong et al., 2010). The dominant vegetation in the wetland are the native Cyperus malaccensis and Phragmites australis, and the invasive Spartina alterniflora. Over the past 10 years, much of the tidal marshes have been converted to aquacultural ponds (Yang et al., 2017a).

2.2. Aquaculture pond management

Small and shallow aquaculture ponds (area of 0.8−2.5 ha and depth of 1.1−1.8 m) are a key feature in the MRE, covering an area of around 234 ha in the Shanyutan Wetland (Yang et al., 2017b). Aquaculture production, which is concentrated between June and November, yields a single annual crop of shrimps from the semi-intensive earthen ponds, which are filled with salt water (average salinity of 2.0− 8.5‰) from the MRE using a submerged pump. The shrimps are fed twice a day (at 07:00 and 16:00 hr) with commercial aquatic feed pellets containing 42% protein. Three to five 1500 W paddlewheel aerators operate four times a day (07:00–09:00, 12:00–14:00, 18:00–20:00, and 00:00–03:00 hr) to provide sufficient oxygen. This study selected three replicate ponds that were separated by a distance of <10 m (see Table S1 for basic characteristics) (Zhang et al., 2019) for the field measurements. Additional details about

the shrimp pond system and management can be found in Yang et al. (2017b).

2.3. Determination of dissolved CH4 concentration

Field sampling campaigns were carried out at three aquaculture ponds between June and November 2017 following the main aquaculture practice. In each pond, a wooden bridge was built reaching ~10 m from the pond embankment to the pond center in order to conveniently collect the water and gas samples at three sites. Samples were collected two or three times each month in the three aquaculture ponds. Overall, sampling was conducted for 15 different times. The total number of samples was 3 ponds × 3 sites × 15 times = 135. To measure the dissolved CH4 concentrations, surface water (at a depth of ~20 cm) was collected using a homemade water sampler and transferred into a 55-mL gas-tight glass serum bottle that had been flushed with pond water for 2-3 times. After being completely filled, the glass bottles were immediately sealed with a butyl rubber stopper using an aluminum screw cap, ensuring that all air bubbles were excluded. To inhibit bacterial activity, 0.2 mL of saturated HgCl2 solution was added to each bottle of water sample (Borges et al., 2018; Hu et al., 2018). Samples were transported back to the laboratory in an ice-packed cooler. Dissolved CH4 concentrations of the samples were measured within 2 d of collection following the headspace equilibration method. Approximately 25 mL headspace was created by injecting ultra-high purity N2 gas (>99.999%) into the glass bottle, while simultaneously 25 mL water sample was withdrawn. The bottle was then shaken vigorously for 20 min and left at room temperature for 30 min to form a complete equilibration between the air and water phases (Cotovicz et al., 2016). Approximately 10 mL of the equilibrated headspace air was subsequently extracted and injected into a gas chromatograph (GC-2010, Shimadzu, Kyoto, Japan) equipped with a flame ionization detector (FID) to determine the CH4 concentrations. Standard CH4 gases at five concentrations, namely 2, 8, 500, 1000, and 10,000 ppm, were

used to calibrate the FID of gas chromatograph. Dissolved CH4 concentrations of the sample were calculated based on the volume of water, headspace air in the sampling glass bottle, and gas solubility coefficient that was a function of water temperature and salinity (Farías et al., 2017; Wanninkhof, 1992; Xiao et al., 2017).

2.4. Determination of diffusive CH4 flux across the water-air interface

2.4.1. Measurement using floating chambers

The floating chamber methods (FCs) are one of the foremost techniques for directly measuring CH4 emissions from aquatic ecosystems (e.g., Chuang et al., 2017; Gålfalk et al., 2013; Welti et al., 2017). In order to measure the diffusive CH4 effluxes from the aquaculture ponds, this study used a modified chamber placed on a floating buoy (Figure S2). The opaque floating chambers were made from inverted plastic basin (polyethylene/plexiglas®) with a volume and area of 5.2 L and 0.1 m2, respectively. The chambers were covered with aluminum tape to minimize internal heating by sunlight (Natchimuthu et al., 2016; Yang et al., 2019). Thin gauze (bore diameter 0.001 mm) was used to cover the FCs aperture to minimize the entry of bubbles into the chamber (Figure S2). A fan was installed inside the chamber to mix the headspace air during the gas sampling. In order to quantify the potential contribution of CH4 ebullition flux from the aquaculture ponds, total CH4 fluxes were also determined by using floating chamber without gauze.

CH4 fluxes were measured over a period of 45 min, with four headspace air samples being collected inside the chamber at 15-min interval using 60-mL plastic syringes equipped with three-way stopcocks. The gas samples were immediately transferred into pre-evacuated airtight gas sampling bags (Dalian Delin Gas Packing Co., Ltd., China), transported to the laboratory, and analyzed within 48 h using a gas

chromatograph (GC-2010, Shimadzu, Kyoto, Japan) equipped with a FID, following the method of Tong et al. (2010). The detection limits for CH4 were 0.3 ppm, and the relative standard deviations of CH4 analyses were ≦2.0% in 24 h.

CH4 emission fluxes (FCH4, μmol m−2 hr−1) were calculated based on the slope of the regression between headspace CH4 concentration and time (Yang et al., 2019). Generally, if r2 of the correlation between headspace CH4 concentration and the elapsed time is larger than 0.90, the CH4 emission is considered as diffusion only (Bastviken et al., 2010; Zhu et al., 2016). If r2 is below 0.90, the emission is considered as the combination of ebullition and diffusion. The floating chambers with gauze (FCs-G) and without gauze (FCs-NG) showed distinct linear ($r2>0.9$) and nonlinear ($r2<0.9$) increases in methane concentration, and therefore the contribution of ebullition was calculated by the difference of the diffusion flux measured between the FCs-G and the FCs-NG methods.

2.4.2. Estimation using thin boundary layer models

Saturation (S) of CH4 in pond water was the ratio between the in situ dissolved concentration of CH4 in pond water and the calculated saturated CH4 concentration corresponding to ambient air CH4 concentration (Hu et al., 2018) (Eq. 1):

$$S = Cwater/CWs = Cwater/(\alpha \times Cair) \times 100\% \quad \text{(Eq. 1)}$$

where Cwater is dissolved CH4 concentration in pond water; CWs is the saturated CH4 concentration (μmol L−1); Cair is the atmospheric concentration (μmol mol-1) of the sampling sites; and α is the Bunsen coefficient (Wanninkhof, 1992).

Diffusive fluxes of CH4 (F, μmol m−2 hr−1) across the water-air interface can be described by using a theoretical diffusion model (Eq. 2) (Musenze et al., 2014):

176 $$F = k \times (C_{water} - C_{eq})$$ (Eq. 2)

177 where Cwater (μmol L-1) is the measured dissolved CH4 concentration in surface water, Ceq (μmol L-1) is
178 the dissolved CH4 concentration in equilibrium with the air above, and k is the gas transfer velocity (cm
179 h-1). The k value was parameterized as a function of wind speed and normalized for surface water
180 temperature (T, oC) using a Schmidt number (Sc) derived from Eq. 3:

181 $$Sc = 2039.20 - 120.31T + 3.4209T^2 - 0.040437T^3$$ (Eq. 3)

182 This study evaluated the variations in CH4 fluxes across the water-air interface estimated by eight widely
183 used wind-based models developed in various conditions, including wind tunnels, open sea, estuarine
184 systems, and lakes, as follows:

185 LM86 (Liss and Merlivatt 1986)

186 $$F_{LM86} = 0.17U_{10}(Sc/600)^{-2/3}(C_{water} - C_{eq}) \qquad 0 < U_{10} \leqq 3.6$$ (Eq. 4)

187 $$F_{LM86} = (2.85U_{10} - 9.65)(Sc/600)^{-1/2}(C_{water} - C_{eq}) \qquad 3.6 < U_{10} \leqq 13$$ (Eq. 5)

188 W92a (Wanninkhof, 1992)

189 $$F_{W92a} = 0.31U_{10}^2(Sc/660)^{-1/2}(C_{water} - C_{eq})$$ (Eq. 6)

190 RC01 (Raymond and Cole, 2001)

191 $$F_{RC01} = 1.91exp(0.35U_{10})(Sc/600)^{-1/2}(C_{water} - C_{eq})$$ (Eq. 7)

192 CL98 (Cole & Caraco, 1998)

193 $$F_{CL98} = [2.07 + (0.215 \times U_{10}^{1.7})](Sc/600)^{-2/3}(C_{water} - C_{eq})$$ (Eq. 8)

194 W92b (Wanninkhof, 1992)

$$F_{W92b} = 0.45U_{10}^{1.64}(Sc/600)^{-1/2}(C_{water} - C_{eq}) \quad \text{(Eq. 9)}$$

CW03 (Crusius & Wanninkhof, 2003)

$$F_{CW03} = 0.72U_{10}(Sc/600)^{-2/3}(C_{water} - C_{eq}) \qquad U_{10} < 3.7 \quad \text{(Eq. 10)}$$

$$F_{CW03} = (4.33U_{10} - 13.3)(Sc/600)^{-1/2}(C_{water} - C_{eq}) \qquad U_{10} \geq 3.7 \quad \text{(Eq. 11)}$$

where U10 was determined according to the logarithmic wind profile relationship using Eq. 12 (Crusius and Wanninkhof, 2003):

$$U_{10} = U_z[1 + \frac{(C_{d10})^{1/2}}{K}\ln(\frac{10}{z})] \quad \text{(Eq. 12)}$$

where Uz is the wind speed (m s-1) at height z above the water surface (2.5 m in this study), Cd10 is the drag coefficient at 10 m above the water surface (0.0013 m s-1), and K is the von Karman constant (0.41). Generally, the stability of the atmosphere was an important factor influencing the calculation of U10 using the wind-based equations. If the atmosphere over the aquatic systems is unstable, and the equation used to calculate U10 needs to be adjusted. The air-water temperature difference can be used to determine if the atmosphere over the aquatic systems is stable or not. If the air-water temperature difference is positive, the atmosphere over the aquatic systems is stable. In the present study, the air temperature in ponds were higher than water temperature during the study period, with the air-water temperature difference period ranged from 0.1 to 3.8 oC, indicating that the atmosphere over the ponds is neutral stability regime. Therefore, no adjustment is needed for U10, and the equation (12) was appropriate for the calculation of U10. Some recent studies have applied surface renewal models that take into account both wind speed and buoyancy to determine the k values (e.g., Czikowsky et al., 2018; MacIntyre et al., 2010; MacIntyre et al., 2018).

2.5. Measurement of meteorological and environmental variables

Meteorological variables, including air temperature (AT), air pressure (AP), wind speed (WS), and precipitation, were recorded at 30-min intervals using an automatic meteorological station (Vantage Pro 2, China) installed at the MRE weather station in the China Wetland Ecosystem Research Network. The distance between the automatic meteorological station and sampling ponds is about 75 m. The precision for air temperature, atmospheric pressure, and precipitation were ± 0.2 °C, ± 1.5 hPa, and ± 0.4 mm min-1, respectively (Yang et al., 2020). The air temperature and wind speed were sampled at 1 Hz. WS were determined using a cup anemometer that was connected to a Anemometer Sensors that registered the wind speed in 1.0 m s-1 bins at 1-min interval. The threshold for startup of the anemometer was 0.4 m s-1. Approximately 6% of wind speed measurements during the study period were below the threshold of 0.4 m s-1 at 2.5 m height.

Water temperature, electrical conductivity (EC), pH, dissolved oxygen (DO), total organic carbon (TOC), and total dissolved nitrogen (TDN) content of surface water (~20 cm below the water surface) were recorded at the three study sites in all 15 sampling campaigns. Water temperature and pH were measured using a portable pH/mV/Temperature meter (IQ150, IQ Scientific Instruments, USA), and EC and DO were determined using an electrical conductivity meter (2265FS EC, Spectrum Technologies, USA) and a multiparameter water quality probe (550A YSI, USA), respectively. The relative standard deviations of EC, pH, and DO analyses were ≦1.0%, ≦1.0% and ≦2.0%, respectively

Water samples for TOC and TDN analyses were collected using a 5-L plexiglass hydrophore, transferred to a 150-mL polyethylene bottle, and then transported to the laboratory in an ice-packed cooler. TOC and N-NOx- (NO2- + NO3-) concentrations were analyzed, after filtering through a 0.45-μm

cellulose acetate filter (Biotrans nylon membranes), using a TOC analyzer (TOC-VCPH/CPN, Shimadzu, Kyoto, Japan) and a flow injection analyzer (Skalar Analytical SAN++, The Netherlands), respectively. The detection limits for N-NOx− and TOC were 6 μg L-1 and 4 μg L-1, respectively. The relative standard deviations of N-NOx− and TOC analyses were ≦3.0% and ≦1.0%, respectively.

2.6. Statistical analysis

Repeated-measures analysis of variance (RMANOVA) was conducted to test the differences in diffusive CH4 fluxes between the two approaches over the study period. Pearson correlation analyses were conducted to examine the relationships between (1) dissolved CH4 concentration or CH4 fluxes and environmental variables, and (2) diffusive CH4 fluxes measured using *FCs* and estimated using the gas transfer velocity models. The coefficient of variation (CV) for CH4 fluxes on each sampling campaign was determined by dividing the standard deviation by the mean value. Statistical analyses were conducted using software SPSS (v. 17.0, SPSS Inc., USA) at a significance level of 0.05. Data are presented as mean ± 1 standard error.

Generalized linear modelling was conducted to determine the variables that influenced CH4 emission fluxes from these seven different methods (i.e. FCs + 8 TBL models). The “gls” function from the “nlme” R package (Pinheiro et al., 2018) with a saturated model was conducted for all variables (dissolved CH4, U10, water temperature, dissolved oxygen, total dissolved carbon and dissolved nitrate). This model was run using the stepAIC function in R “MASS” package that follows the Akaike Information Criterion (AIC) (Venables and Ripley, 2002). It can identify the best model (lowest AIC value) in each case.

3. Results

3.1. Meteorological and environmental variables

The average air temperature (AT) and air pressure (AP) during the research period were 28.7±0.4 °C (range: 18.6−35.6 °C) and 1010.0±0.5 hPa (range: 985−1025 hPa), respectively. Notably, the maximal AT appeared in July and the minimal AP happened in August, very different from other months. The WS during the study period ranged from 0.2 to 18.8 m s-1, and varied between seasons, with a peak in July (Figure S3a). Approximately 92% of WS fell within the range of 0.2−4.0 m s-1 (Figure S3b).

There were also clear temporal variations in surface water characteristics during the study period. The mean water temperature ranged from 18.1 °C (November) to 34.4 °C (August) (Figure S4a), while the mean DO concentration changed between 9.4 mg L-1 (August) and 19.9 mg L-1 (November) (Figure S4). The mean TOC concentrations varied between 9.9 mg L-1 (July) and 57.3 mg L-1 (November) (Figure S3), while N-NOx- concentrations ranged from 504 μg N L-1 (June) to 10.7 μg N L-1 (November) (Figure S4).

3.2. Model estimated k values and dissolved CH4 concentrations

The mean k values showed considerable variations between different models and decreased in the order: kRC01 (6.5±0.8 cm h-1) > kW92a (3.5±0.7 cm h-1) > kFCs (3.2±0.4 cm h-1) > kCL98 (2.9±0.3 cm h-1) > kCW03 (2.5±0.5 cm h-1) > kW92b (2.4±0.4 cm h-1) > kLM86 (0.6±0.1 cm h-1) (Figure 1).

Dissolved CH4 concentrations demonstrated large variations over the study period (0.1−31.1 μmol L-1), and they increased first and decreased to a valley later (Figure 2). CH4 concentrations were supersaturated across all ponds and all sampling dates, with an overall mean of 4.8 ± 0.8 μmol L-1 (162.0 ±18.4 ppmv), equivalent to 8700% saturation (range of 200–5.9 × 104% saturation).

3.3. CH4 flux estimates by using TBL models and FCs method

There were considerable differences in the estimated diffusive CH4 fluxes among

277 the *TBL* models (*TBL*RC01: 215.9 ± 39.2 μmol m−2 h−1; *TBL*CL98:
278 115.0 ± 21.9 μmol m−2 h−1; *TBL*W92a: 102.9 ± 19.5 μmol m−2 h−1; *TBL*W92b:
279 78.3 ± 13.9 μmol m−2 h−1; *TBL*CW03: 74.9 ± 13.2 μmol m−2 h−1; and, *TBL*LM86:
280 19.5 ± 3.7 μmol m−2 h−1) (Table 1, Fig. 3 and Figure S5). Although there were marked
281 variations in the flux estimates among the various models, results from all models showed
282 similar temporal patterns (Fig. 3). The largest fluxes were generally recorded between August
283 and October, while the lowest fluxes were consistently recorded in June and November (Fig.
284 3).

285 Direct measurements using *FCs* with gauze (*FCs*-G) and without gauze (*FCs*-NG)
286 methods were 75.0 ± 12.5 (Fig. 3) and 231.3 ± 681.3 μmol m−2 h−1 (Figure S6; Yang et al.,
287 unpublished data), showing significant difference between the two methods (Independent
288 Samples T-Test, $F = 118.190$, $p < 0.001$). On average, ebullitive CH4 flux accounted for
289 33%–99% of the total CH4 emissions during the study period.

290 3.4. Environmental influences on dissolved CH4 concentrations and fluxes

291 Pearson correlation analysis showed that dissolved CH4 concentrations in the shrimp ponds were
292 significantly positive correlated with air temperature and TOC concentration ($p<0.01$), and negatively
293 corelated with N-NO3− concentration and EC ($p<0.01$) (Table 2). CH4 fluxes were found to be positively
294 correlated with air temperature ($p<0.05$), TOC concentration and dissolved CH4 concentration ($p<0.01$),
295 and negatively correlated with water N-NO3− concentration ($p<0.01$) and EC ($p<0.05$) (Table 2 and Table
296 S3). This study also analyzed the relationships between the CH4 fluxes derived from the seven different
297 methods and various environmental variables. N-NO3- concentration was consistently and negatively

298 correlated with CH4 fluxes (Table S2). Environmental variables explained a larger proportion of variability
299 in CH4 fluxes derived from the six TBL models (R2=0.46-0.54) than those from direct FCs measurements
300 (R2=0.35) (Table S2).

301 4. Discussion

302 4.1. CH4 supersaturation and degassing from aquaculture ponds

303 There are few studies on CH4 concentrations in small ponds, particularly, those created for
304 aquaculture purposes. In this study, the dissolved CH4 concentration in surface water of the aquaculture
305 ponds ranged from 0.14 to 31.13 μmol L-1 during the study period. The CH4 concentration in our ponds
306 were higher than those observed in many small ponds in Florida (~2.2 μmol L-1; Barber et al., 1988),
307 Colorado (~1.0 μmol L-1; Bastviken et al., 2004), and Wisconsin and Minnesota (0.3−2.3 μmol L-1; Smith
308 and Lewis, 1992) in the USA, in Sweden (~1.3 μmol L-1; Natchimuthu et al., 2014), Canada (0.5−6.7
309 μmol L-1; Pelletier et al., 2014), and Siberia (~2.6 μmol L-1; Repo et al., 2007). In addition, CH4
310 concentration in our researched aquaculture ponds were generally larger than those in some
311 nutrient-enriched rivers in China, i.e. Lixiahe River (0.2−0.81 μmol L-1; Wu et al., 2019), and Beitang
312 Drainage River and Dagu Drainage River (0.3−1.7 μmol L-1; Hu et al., 2018). Similar to inland aquatic
313 systems, such as lakes (e.g., Wen et al., 2016; Wik et al., 2016; Yan et al., 2018), reservoirs (e.g., Deemer
314 et al., 2016; Musenze et al., 2014; Wang et al., 2017), rivers (e.g., Barbosa et al., 2016; Striegl et al., 2012),
315 floodplains (Barbosa et al., 2020) and small ponds (e.g., Holgerson and Raymond, 2016; Wik et al., 2016),
316 aquaculture ponds were supersaturated for CH4 (range of 2.71−599.81 folds supersaturation) with respect
317 to the atmospheric equilibrium (Figure 2b). The small temporary ponds in the Yale Myers Forest in
318 Connecticut, the USA, have, until now, the highest concentrations of CH4, with the range of 21.0−58.9

μmol L-1, equal to 119.0−2906.6 folds supersaturation (Holgerson, 2015). The CH4 concentrations and supersaturations in our aquaculture ponds fall well within the range reported previously by Holgerson (2015). Our results indicated that aquaculture ponds in the subtropical estuaries were hotspots for CH4 emission.

In inland aquatic ecosystems, the strong CH4 release is likely a result of large organic matter input from the catchment that sustains high methanogenic rates (Finlay et al., 2009; Lundin et al., 2013; Venkiteswaran et al., 2013; Yan et al., 2018), which is supported by the significant relationship between dissolved CH4 and nutrient level (Huttunen et al., 2003; Kortelainen et al., 2001; Wen et al., 2016). In this study, aquaculture shrimp ponds were semi-artificial ecosystems that were maintained through a daily feed supply for the production of aquatic animals. However, only a small portion of the feed input was actually converted into shrimp biomass, with the feed utilization efficiency of ~4.0−27.4% (Chen et al., 2016; Molnar et al., 2013; Yang et al., 2017b). Surface sediments in the aquaculture systems typically retain a large amount of organic matter from feces and residual feeds (Chen et al., 2016; Yang et al., 2017b) that can support high levels of CH4 production and its subsequent release to atmosphere. Although organic matter content was not quantified in this study, our results confirmed the significantly positive correlation between dissolved CH4 and TOC concentration ($p<0.01$; Table 2), which lent support to the idea that CH4 supersaturation in the aquaculture ponds was related to the large input of organic matter.

4.2. Comparison of six different TBL modelled CH4 fluxes

Although previous studies have compared the performance of different TBL models in estimating diffusive CH4 fluxes in inland waters (Amouroux et al., 2002; Li et al., 2015; Musenze et al., 2014; Xiao et al., 2017; Zappa et al., 2007), such comparison is scarce for shallow ponds, particularly those created for

aquaculture. To the best of our knowledge, this study is the first attempt to compare the estimates of diffusive CH4 flux using different TBL models over the whole aquaculture period in aquaculture ponds. Interestingly, although the patterns of temporal variations in diffusive CH4 fluxes in the shrimp ponds were largely consistent across the TBL models (Figure 3), there were differences in the magnitude of fluxes estimated from different models (Table 1).

Notably, the mean flux estimate using the TBLRC01 model (215.6 μmol m-2 h-1) was an order of magnitude greater than that derived from the TBLLM86 model (19.4 μmol m-2 h-1, Figure 3). Moreover, CH4 fluxes estimated using the TBLRC01 model were 2 - 3 folds larger than those using the TBLW92a, TBLCL98, TBLW92b, and TBLCW03 models (Table 1 and Figure S5). However, there were no significant differences in mean fluxes between the TBLW92a and TBLCL98 models ($p>0.05$; Table 1 and Figure S5), as well as between the TBLW92b and TBLCW03 models ($p>0.05$; Table 1 and Figure S5). Inland waters (river and reservoirs), similarly, Gao et al. (2014) and Musenze et al. (2014) found that the estimated diffusive CH4 fluxes derived from the TBLRC01 model were substantially greater than those from other TBL models. These results indicated a potential bias in diffusive CH4 flux estimation when only a single TBL model was used. As Musenze et al. (2014) suggested, the lack of consensus among the existing TBL models might be a major source for the uncertainty in GHGs accounting.

The difference of the estimated CH4 fluxes between TBL models was likely a result of the variation in weighting wind as a driver of gas transfer velocity (Musenze et al., 2014, Figure 1). Since these wind-based models were developed using a range of techniques under different conditions in specific systems (Gao et al., 2014; Musenze et al., 2014), their generalized applicability could be limited by the local conditions (Bade, 2009; Musenze et al., 2014; Schilder et al., 2013). Therefore, the TBLCL98 and

TBLCW03 are more appropriate wind-based models for estimating k value and CH4 fluxes in aquaculture ponds, due to that their experiment environments (e.g., lentic ecosystem, a range of wind speeds) were closest to the studied aquaculture ponds. Obviously, more in situ measurement is still needed to further increase the accuracy of the estimate.

4.3. Comparison of CH4 fluxes derived from FCs measurement and TBL models

Previous studies have shown that CH4 fluxes estimated by *TBL* models tend to be lower than those measured by *FCs* (Chuang et al., 2017; Duchemin et al., 1999; Li et al., 2015; Matthews et al., 2003). This study also compared CH4 fluxes measured by *FCs* and those estimated by *TBL* models over the aquaculture season (Table 1 and Figure S5). Although there were significant correlations between *TBL* model estimates and *FCs* measurements ($p < 0.05$ in all cases), the agreement between the two methods varied considerably between models (Fig. 4). The *TBL*W92b and *TBL*CW03 models gave the largest $r2$ values (0.82 and 0.83, respectively) and good agreements with *FCs* measurements (slope = 0.92 and 0.89, respectively), whereas *TBL*CL98 yielded mean estimates virtually identical to *FCs* measurements (slope = 1) but with larger variability around the mean ($r2 = 0.53$) (Fig. 4d–f). In contrast, *TBL*LM86 vastly underestimated FCs fluxes whereas *TBL*RC01 grossly overestimated FCs fluxes (Fig. 4a and b). Approximately 80% of the diffusive CH4 fluxes estimated by the models fell within the range measured by the *FC* method (see Fig. 5).

Balancing the consideration of overall agreement (regression slope) and estimate variability (regression $r2$), the *TBL*W92b and *TBL*CW03 models appeared to give the best

approximations of *FCs* measurements. While previous studies showed that *FCs* were more appropriate for determining greenhouse gas fluxes in heterogeneous environments such as lakes and reservoirs (Cole et al., 2010; Duchemin et al., 1999; Murray et al., 2015; Vachon et al., 2010; Wu et al., 2018), our results suggest that *TBL*W92b and *TBL*CW03 models are reliable alternatives for estimating CH4 diffusive flux in shallow aquaculture ponds.

In addition to diffusive flux from the water column, bottom sediment could also contribute to CH4 emission via ebullition, especially in eutrophic, shallow aquaculture ponds. This is illustrated by the differences in the measured CH4 flux using *FCs* with and without gauze in our aquaculture ponds (Figure S6). The CH4 flux measured by *FCs* without gauze (2231.3 ± 681.3 μmol m−2 h−1) were one to two orders of magnitude higher than that by *FCs* with gauze (75.0 ± 12.5 μmol m−2 h−1) (Figure S6); from this ebullition was estimate to contribute 96.6% to the total CH4 emissions. Overall, our results showed that ebullition was the primary path of CH4 emission in aquaculture ponds, and that ebullitive flux vs. diffusive flux could be easily resolved with a simple design of *FCs* with a detachable gauze.

4.4. Implications of the comparison between different methods

The *FCs* method is the popular technique for measuring CH4 emissions due to its ability to detect low fluxes and the simplicity of its operating principle (Bastviken et al., 2015; Lorke et al., 2015; Musenze et al., 2014; Podgrajsek et al., 2014). However, the *FCs* method requires time-consuming manual operation, which limits the frequency of measurements and can be difficult to deploy in remote areas (Acosta et al., 2017; Morin et al., 2017). Improvement of the

global CH4 budget would require high-resolution emission data covering large time and spatial scales, which obviously is difficult to achieve with the *FCs* method.

Large-scale estimates of aquatic CH4 emissions using *TBL* models has been gaining popularity (Holgerson and Raymond, 2016; Martinez-Cruz et al., 2016; Musenze et al., 2014; Wang et al., 2017) due to their simplicity, practicality and low cost. There are, however, different *TBL* models to choose from, and the large differences in the model performances (Fig. 4) mean that selecting the appropriate model(s) would be critical, or otherwise large errors would occur when upscaling the results from small ponds to the regional/global scale. Our results suggest that *TBL*W92b and *TBL*CW03 models could be used as effective and convenient alternatives to *FCs* in shallow aquaculture ponds.

4.5. Limitation and future research

The *FCs* method is a common method to measure CH4 fluxes from aquatic ecosystems. However, *FCs* may create microenvironments that affect the boundary layer conditions through, for instance, blockage of wind, change of atmospheric pressure at the measurement point, and change in the gas transfer rate through pressure build-up (Duchemin et al., 1999; Matthews et al., 2003; Musenze et al., 2014). For example, the turbulence resulted from the chamber walls can enhance the efficiency of gas exchange and increase gas fluxes during low wind conditions (Matthews et al., 2003; Xiao et al., 2016).

TBL models rely on the gas transfer velocity coefficient (*kx*), which itself is estimated from some empirical wind-based models. Effects of artificial aeration, which is commonly done in aquaculture ponds, on *kx* are unknown. More importantly, the *TBL* models ignore the effect of

buoyancy fluxes near the air-water interface on *kx*. An alternative is the surface renewal model (SRM), which considers both wind speed and buoyancy (e.g., Czikowsky et al., 2018; MacIntyre et al., 2010; MacIntyre et al., 2018).

The use of eddy covariance (EC) technique is increasingly popular as it can provide a better characterization of the variation in CH4 fluxes through quasi-continuous measurements (Acosta et al., 2017; Morin et al., 2017; Xiao et al., 2014; Zhao et al., 2019). However, its application in small water bodies (e.g., ponds) is limited by footprint contamination (Zhao et al., 2019). Developing a practical and effective way to reduce the flux footprint and the contamination from gaseous sources outside the water body will allow broader application of EC method in the future.

Different methods have their own limitations; careful comparison and cross calibration would be needed to increase the overall accuracy of these methods and to improve the global CH4 budget.

5. Conclusions

Despite the large CH4 emission from ponds, there is limited information about the comparison between different methods applied for the estimations of CH4 fluxes across the water-air interface. In this study, FCs and six TBL models were applied to estimate CH4 fluxes from aquaculture ponds. Our results indicate that dissolved CH4 concentrations in the subtropical shallow aquaculture ponds were on average ~87 times more oversaturated than the ambient air, and thus the pond surfaces acted as considerable atmospheric CH4 sources. The high organic matter loading contributed to the CH4 supersaturated in the aquaculture ponds. As the first attempt in aquaculture ponds, this study also compared the CH4 fluxes

444 directly measured by using floating chambers (FCs) and estimated by six thin boundary layer (TBL)
445 models (TBLLM86, TBLW92a, TBLRC01, TBLCL98, TBLW92b, and TBLCW03). The diffusive CH4
446 fluxes estimated by different TBL models were largely variable, but overall they were 27 - 300% larger
447 than those directly measured by FCs. The agreement between FCs-measured and model-estimated CH4
448 fluxes was highest for the TBLW92b, TBLCW03 models. While our results suggested that the estimation
449 of CH4 fluxes using a single TBL model could lead to high levels of uncertainty, the application of
450 TBLW92b and TBLCW03 models could provide a robust and simple way for characterizing CH4 fluxes
451 over direct measurements using FCs. Our results suggest that the comparison of different methods and
452 selection of the most appropriate method(s) for determining CH4 flux should be a top research priority to
453 improve the estimation accuracy of GHGs fluxes in aquaculture ponds and other aquatic ecosystems.

454 Declaration of competing interest

455 The authors declare that they have no known competing financial interests or personal relationships
456 that could have appeared to influence the work reported in this paper.

457 Acknowledgments

458 This research was financially supported by the National Science Foundation of China (grant numbers
459 41801070 and 41671088), National Key Research & Development Plan "Strategic International Scientific
460 and Technological Innovation Cooperation" (2016YFE0202100), Council of the Hong Kong Special
461 Administrative Region, China (CUHK458913 and CUHK Direct Grant SS15481), Spanish Government
462 (grant CGL2016-79835), Catalan Government (grant SGR 2017-1005), European Research Council
463 (Synergy grant ERC-SyG-2013-610028), Open Research Fund Program of Jiangsu Key Laboratory of
464 Atmospheric Environment Monitoring & Pollution Control (grant KHK1806), Priority Academic Program

Development of Jiangsu Higher Education Institutions (PAPD), and Minjiang Scholar Programme. We thank Qianqian Guo, Guanghui Zhao, and Ling Li of the School of Geographical Sciences, Fujian Normal University, for assistance in the field.

References

Acosta, M., Dušek, J., Chamizo, S., Serrano-Ortiz, P., Pavelka, M., 2019. Autumnal fluxes of CH_4 and CO_2 from Mediterranean reed wetland based on eddy covariance and chamber methods. Catena 183, 104191. https://doi.org/10.1016/j.catena.2019.104191

Amouroux, D., Roberts, G., Rapsomanikis, S., Andreae, M.O., 2002. Biogenic gas (CH_4, N_2O, DMS) emission to the atmosphere from near-shore and shelf waters of the north-western Black Sea. Estuar. Coast. Shelf S. 54(3), 575-587.https://doi.org/10.1006/ecss.2000.0666

Bade, D.L., 2009. Gas Exchange at the Air-Water Interface. InEncyclopedia of Inland Waters; Likens, G. E., Ed.; Academic Press:Oxford, pp 70-78.

Barber, T.R., Burke, R.A. Jr., Sackett, W.M., 1988. Diffusive flux of methane from warm wetlands. Global Biogeochem. Cy. 2, 411-425.

Barbosa, P.M., Melack, J.M., Amaral, J.H.F., Scofield, V., Farjalla V., Forsberg, B.R., 2016. Diffusive methane fluxes from Negro, Solimões and Madeira rivers and fringing lakes in the Amazon basin. Limnol. Oceanogr. 61, S221-237. https://doi.org/10.1002/lno.10358

Barbosa, P.M., Melack, J.M., Amaral, J.H.F., MacIntyre, S., Kasper, D., Cortes, A.C., Farjalla, V.F., Forsberg, B.R., 2020. Dissolved methane concentrations and fluxes to the atmosphere from a tropical floodplain lake. Biogeochemistry 148, 129-151. https://doi.org/10.1007/s10533-020-00650-1

Bastviken, D., Cole, J., Pace, M., Tranvik, L., 2004. Methane emissions from lakes: Dependence of lake characteristics, two regional assessments, and a global estimate. Global Biogeochem. Cy. 18, GB4009. https://doi.org/10.1029/2004GB002238

Bastviken, D., Santoro, A.L., Marotta, H., Pinho, L.Q., Calheiros, D.F., Crill, P., Enrich-Prast, A., 2010. Methane emissions from Pantanal, South America, during the low water season: Toward more comprehensive sampling. Environ. Sci. Technol. 44,5450-5455.

491 Bastviken, D., Tranvik, L.J., Downing, J.A., Crill, P.M., Enrich-Prast, A., 2011. Freshwater methane
492 emissions offset the continental carbon sink. Science 331, 50.

493 Bastviken, D., Sundgren, I., Natchimuthu, S., Reyier, H., Gålfalk, M., 2015. Cost-efficient approaches to
494 measure carbon dioxide (CO_2) fluxes and concentrations in terrestrial and aquatic environments using
495 mini loggers. Biogeosciences 12(12), 3849-3859. https://doi.org/10.5194/bg-12-3849-2015

496 Borges, A.V., Speeckaert, G., Champenois, W., Scranton, M.I., Gypens, N., 2018. Productivity and
497 temperature as drivers of seasonal and spatial variations of dissolved methane in the Southern Bight of
498 the North Sea. Ecosystems 21(4), 583-599. https://doi.org/10.1007/s10021-017-0171-7

499 Chen, Y., Dong, S.L., Wang, F., Gao, Q.F., Tian, X.L., 2016. Carbon dioxide and methane fluxes from
500 feeding and no-feeding mariculture ponds. Environ. Pollut. 212,
501 489-497.http://dx.doi.org/10.1016/j.envpol.2016.02.039

502 Chuang, P.-C., Young, M.B., Dale, A.W., Miller, L.G., Herrera-Silveira, J.A., Paytan, A., 2017. Methane
503 fluxes from tropical coastal lagoons surrounded by mangroves, Yucatán, Mexico. J. Geophys. Res.
504 Biogeosci., 122(5), 1156-1174. https://doi.org/10.1002/2017JG003761

505 Cole, J.J., Caraco, N.F., 1998. Atmospheric exchange of carbon dioxide in a low-wind oligotrophic lake
506 measured by the addition of SF6. Limnol. Oceanogr. 43(4): 647-656.

507 Cole, J.J., Bade, D.L., Bastviken, D., Pace, M.L., Van de Bogert, M., 2010. Multiple approaches to
508 estimating air-water gas exchange in small lakes. Limnol. Oceanogr. Methods 8,
509 285-293.https://doi.org/10.4319/lom.2010.8.285

510 Cotovicz Jr., L.C., Knoppers,B.A., Brandini,N., Poirier,D., Costa Santos,S.J., Abril, G., 2016.
511 Spatio-temporal variability of methane (CH_4) concentrations and diffusive fluxes from a tropical
512 coastal embayment surrounded by a large urban area (Guanabara Bay, Rio de Janeiro, Brazil). Limnol.
513 Oceanogr.61(S1), 238-252. https://doi.org/10.1002/lno.10298

514 Crusius, J., Wanninkhof, R., 2003. Gas transfer velocities measured at low wind speed over a lake. Limnol.
515 Oceanogr. 48(3), 1010-1017.

516 Czikowsky, M.J., MacIntyre, S., Tedford, E.W., Vidal, J., Miller, S.D., 2018. Effects of wind and buoyancy
517 on carbon dioxide distribution and air-water flux of a stratified temperate lake. J. Geophys.
518 Res.-Biogeo. 123, 2305-2322. https://doi.org/10.1029/2017JG004209

519 Deemer, B.R., Harrison, J.A., Li, S.Y., Beaulieu, J.J., Delsontro, T., Barros, N., Bezerra-Neto, J.F., Powers,
520 S.M., dosSantos, M.A., Vonk, J.A., 2016. Greenhouse gas emissions from reservoir water surfaces: A
521 New Global Synthesis. Bioscience 66(11), 949-964. https://doi.org/10.1093/biosci/biw117

522 Denmead, O.T., 2008. Approaches to measuring fluxes of methane and nitrous oxidebetween landscapes
523 and the atmosphere. Plant Soil 309, 5-24.https://doi.org/10.1007/s11104-008-9599-z

524 Descloux, S., Chanudet, V., Serça,D., Guérin, F., 2017. Methane and nitrous oxide annual emissions from
525 an old eutrophic temperate reservoir. Sci. Total Environ. 598,
526 959-972.http://dx.doi.org/10.1016/j.scitotenv.2017.04.066

527 Duchemin, E., Lucotte, M., Canuel, R., 1999. Comparison of static chamber and thinboundary layer
528 equation methods for measuring greenhouse gas emissionsfrom large water bodies. Environ. Sci.
529 Technol. 33, 350-357. http://dx.doi.org/10.1021/es9800840

530 FAO, 2017. Fishery and aquaculture statistics (global aquaculture production 1950-2014). FishStatJ.
531 http://www.fao.org/fishery/statistics/software/fishstatj/en.

532 Farías, L., Sanzana, K., Sanhueza-Guevara, S., Yevenes, M.A., 2017. Dissolved methane distribution in the
533 Reloncaví Fjord and adjacent marine system during austral winter (41°-43° S). Estuar. Coast. 40(6),
534 1592-1606. https://doi.org/10.1007/s12237-017-0241-2

535 Finlay, K., Leavitt, P.R., Wissel, B., Prairie, Y.T., 2009. Regulation of spatial andtemporal variability of
536 carbon flux in six hard-water lakes of the Northern GreatPlains. Limnol. Oceanogr. 54, 2553-2564.
537 https://doi.org/10.4319/lo.2009.54.6

538 Gålfalk, M., Bastviken, D., Fredriksson, S., Arneborg, L., 2013. Determination of the piston velocity for
539 water-air interfaces using flux chambers, acoustic Doppler velocimetry, and IR imaging of the
540 water surface. J. Geophys. Res. Biogeosci. 118, 770-782. https://doi.org/10.1002/jgrg.20064

541 Gao, J., Zheng, X.H., Wang, R., Liao, T.T., Zuo, J.W., 2014.Preliminary comparison of the static floating
542 chamber and thediffusion model methods for measuring water−atmosphere exchanges of methane
543 and nitrous oxide from inland water bodies. ClimaticEnviron. Res. 19(3), 290-302. (In Chinese)

Hirota, M., Senga, Y., Seike, Y., Nohara, S., Kunii, H., 2007. Fluxes of carbon dioxide, methane and nitrous oxide in two contrastive fringing zones of coastal lagoon, Lake Nakaumi, Japan. Chemosphere, 68(3), 597-603. https://doi.org/10.1016/j.chemosphere.2007.01.002

Hu, B.B., Wang, D.Q., Zhou, J., Meng, W.Q., Li, C.W., Sun,Z.B., Guo, X., Wang, Z.L., 2018. Greenhouse gases emission from the sewage draining rivers. Sci. Total Environ. 612, 1454-1462. http://dx.doi.org/10.1016/j.scitotenv.2017.08.055

Holgerson, M.A., 2015. Drivers of carbon dioxide and methane supersaturation in small, temporary ponds. Biogeochemistry 124(1-3), 305-318. https://doi.org/10.1007/s10533-015-0099-y

Holgerson, M.A., Raymond, P. A., 2016. Large contribution to inland water CO_2 and CH_4 emissions from very small ponds. Nat. Geosci. 9(3): 222-226. https://doi.org/10.1038/NGEO2654

Hu, Z.Q., Wu, S., Ji, C., Zou, J.W., Zhou, Q.S., Liu, S.W., 2016. A comparison of methane emissions following rice paddies conversion to crab-fish farming wetlands in southeast China. Environ. Sci. Pollut. Res. 23(2),1505-1515. https://doi.org/0.1007/s11356-015-5383-9

Huttunen, J.T., Alm, J., Liikanen, A., Juutinen, S., Larmola, T., Hammar, T., et al., 2003. Fluxes of methane, carbon dioxide and nitrous oxide in boreal lakes and potential anthropogenic effects on the aquaticgreenhouse gas emissions. Chemosphere 52, 609-621.https://doi.org/10.1016/S0045-6535(03)00243-1

IPCC, 2019. In: Calvo Buendia, E., Tanabe, K., Kranjc, A., Baasansuren, J., Fukuda, M., Ngarize, S. (Eds.), 2019 Refinement to the 2006 IPCC Guidelines for National Greenhouse Gas Inventories, Volum 4. IPCC, Switzerland. Kanagawa, Japan Chapter 07.

Jonsson, A., Åberg, J., Lindroth, A., Jansson, M., 2008. Gas transfer rate and CO_2 fluxbetween an unproductive lake and the atmosphere in northern Sweden. J. Geophys.Res. 113, G04006.

Kortelainen, P., Huttunen, J.T., Vaisanen, T., Mattsson, T., Karjalainen, P.,Martikainen, P.J., 2001. CH_4, CO_2 and N_2O supersaturation in 12 Finnish lakesbefore and after ice-melt. In: Williams, W.D. (Ed.), International Association ofTheoretical and Applied Limnology, vol. 27, pp. 1410-1414. Pt 3, Proceedings. 27.

Li, J.H., Pu, J.B., Sun, P.A., Yuan, D.X., Liu, W., Zhang, T., Mo, X., 2015. Summer greenhouse gases exchange flux across water-air interface in three water reservoirs located in different geologic setting in Guangxi, China. Environ. Sci. 36(11), 4032-4042. (In Chinese)

Liss, P.S., Merlivat, L.,1986. Air-Sea gas exchange rates: introduction and synthesis. In The Role of Air-Sea Exchange in Geochemical Cycling. In: Buat-Menard P, (eds.). Reidel: Dordrecht, The Netherlands, pp,´113-129.

Liu, S.W., Hu, Z.Q., Wu, S., Li, S.Q., Li, Z.F., Zou, J.W., 2015. Methane and nitrous oxide emissions reduced following conversion of rice paddies to inland crab-fish aquaculture in southeast China. Environ. Sci. Technol. 50(2), 633-642.https://doi.org/10.1021/acs.est.5b04343

Lorke, A., Bodmer, P., Noss, C., Alshboul, Z., Koschorreck, M., Somlai-Haase, C., Bastviken, D., Flury, S., McGinnis, D.F., Maeck, A., Müller, D., Premke, K., 2015. Technical note: Drifting versus anchored flux chambers for measuring greenhouse gas emissions from running waters. Biogeosciences 12(23), 7013-7024. http://dx.doi.org/10.5194/bg-12-7013-2015.

Lundin, E.J., Giesler, R., Persson, A., Thompson, M.S., Karlsson, J., 2013. Integrating carbon emissions from lakes and streams in a subarcticcatchment. J. Geophys. Res.-Biogeo. 118, 1200–1207. https://doi.org/10.1002/jgrg.20092

Luo, M., Zeng, C.S., Tong, C., Huang, J.F., Yu, Q., Guo, Y.B., Wang, S.H., 2014. Abundance andspeciation of iron across a subtropical tidal marsh of the Min River estuary in the eastChina Sea. Appl. Geochem. 45, 1-13.

MacIntyre, S., Crowe, A.T., Cortés, A., Arneborg, L., 2018. Turbulence in a small arctic pond. Limnol. Oceanogr. 63, 2337-2358. http://dx.doi.org/10.1002/lno.10941

MacIntyre, S., Jonsson, A.J., Jansson, M., Aberg, J., Turney, D., Miller, S., 2010. Buoyancy flux, turbulence, and the gas transfer coefficient in a stratified lake. Geophys. Res. Lett. 37. http://dx.doi.org/10.1029/2010GL044164

Matthews, C.J.D., St. Louis, V.L., Hesslein, R.H., 2003. Comparison of three techniques used to measure diffusive gas exchange from sheltered aquatic surfaces. Environ. Sci. Technol. 37(4), 772-780.https://doi.org/10.1021/es0205838

Morin, T.H., Bohrer, G., Stefanik, K.C., Rey-Sanchez, A.C., Matheny, A.M. and Mitsch, W.J., 2017.

Combining eddy-covariance and chamber measurements to determine the methane budget from a small, heterogeneous urban floodplain wetland park. Agr. Forest Meteorol. 237, 160-170. http://dx.doi.org/10.1016/j.agrformet.2017.01.022

Molnar, N., Welsh, D. T., Marchand, C., Deborde, J., Meziane, T., 2013. Impacts of shrimp farm effluent on water quality, benthic metabolism and N-dynamics in a mangrove forest (New Caledonia). Estuar. Coast. Shelf S. 117, 12-21. https://doi.org/10.1016/j.ecss.2012.07.012

Murray, R.H., Erler, D.V., Eyre, B.D., 2015. Nitrous oxidefluxes in estuarine environments: response to global change.Global Change Biol. 21(9), 3219-3245. https://doi.org/10.1111/gcb.12923.

Musenze, R. S., Grinham, A., Werner, U., Gale, D., Sturm, K., Udy, J., Yuan, Z.G., 2014. Assessing the spatial and temporal variability of diffusive methane and nitrous oxide emissions from subtropical freshwater reservoirs. Environ. Sci. Technol. 48, 14499-14507. https://doi.org/10.1021/es505324h

Natchimuthu, S., Selvam, B.P., Bastviken, D., 2014. Influence of weather variables on methane and carbon dioxide flux from a shallowpond. Biogeochemistry, 119(1-3), 403-413. https://doi.org/10.1007/s10533-014-9976-z

Natchimuthu, S., Sundgren, I., Gålfalk, M., Klemedtsson, L., Crill, P., Danielsson, Å., Bastviken, D., 2016. Spatio-temporal variability of lake CH_4 fluxes and its influence on annual whole lake emission estimates. Limnol. Oceanogr. 61(S1), S13-S26.https://doi.org/10.1002/lno.10222

Natchimuthu, S., Sundgren, I., Gålfalk, M., Klemedtsson, L., Bastviken, D., 2017. Spatiotemporal variability of lake pCO_2 and CO_2 fluxes in a hemiboreal catchment. J. Geophys. Res. Biogeosci. 122, 30-49. https://doi.org/10.1002/2016JG003449

Repo, M.E., Huttunen, J.T., Naumov, A.V., Chichulin, A.V., Lapshina, E.D., Bleuten, W., Martikainen, P.J., 2007. Release of CO_2 and CH_4 from small wetland lakes in western Siberia. Tellus B 59, 788-796.

Pelletier, L., Strachan, I.B., Garneau, M., Roulet, N.T., 2014. Carbon release from boreal peatland open water pools: Implication for the contemporary C exchange. J. Geophys. Res.-Biogeo. 119, JG002423.

Pinheiro, J. et al. nlme: linear and nonlinear mixed effects models.-R package ver. 3.1-137. (2018).

623 Podgrajsek, E., Sahlee, E., Bastviken, D., Holst, J., Lindroth, A., Tranvik, L., Rutgersson, A., 2014.
624 Comparison of floating chamber and eddy covariance measurements of lake greenhouse gas fluxes.
625 Biogeosciences 11(15), 4225-4233. https://doi.org/10.5194/bg-11-4225-2014

626 Raymond, P., Cole, J., 2001. Gas exchange in rivers and estuaries: Choosing a gas transfer velocity. Estuar.
627 Coast. 24(2), 312-317.

628 Schilder, J., Bastviken, D., van Hardenbroek, M., Kankaala, P., Rinta, P., Sto¨tter, T., Heiri, O., 2013.
629 Spatial heterogeneity and lakemorphology affect diffusive greenhouse gas emission estimates oflakes.
630 Geophys. Res. Lett. 40(21), 5752-5756.https://doi.org/10.1002/2013GL057669

631 Schubert, C.J., Diem, T., Eugster, W., 2012. Methane emissions from a small wind shielded lake
632 determined by eddy covariance, flux chambers, anchored funnels, and boundary model calculations: a
633 comparison. Environ. Sci. Technol. 46(8), 4515-4522. https://doi.org/10.1021/es203465x

634 Smith, L.K., Lewis, W.M.Jr., 1992. Seasonality of methane emissions from five lakes and associated
635 wetlands of the Colorado Rockies. Global Biogeochem. Cy. 6,323-338.

636 Striegl, R.G., Dornblaser, M.M., McDonald, C.P., Rover, J.R., Stets, E.G., 2012. Carbon dioxide and
637 methane emissions from the YukonRiver system. Global Biogeochem. Cy. 26, GB0E05.
638 https://doi.org/10.1029/2012GB004306

639 Tangen, B.A., Finocchiaro, R.G., Gleason, R.A., Dahl, C.F., 2016. Greenhouse gas fluxes of a shallow lake
640 in south-central NorthDakota, USA. Wetlands36(4), 779-787.
641 https://doi.org/10.1007/s13157-016-0782-3

642 Tong, C., Wang, W.Q., Zeng, C.S., Marrs, R., 2010. Methane emissions from a tidal marsh in the Min
643 River estuary, southeast China. J. Environ. Sci. Heal. A. 45,
644 506-516.https://doi.org/10.1080/10934520903542261

645 Vachon, D., Prairie, Y.T., Cole, J.J., 2010. The relationship between near-surface turbulence and gas
646 transfer velocity in freshwatersystems and its implications for floating chamber measuiements of gas
647 exchange. Limnol. Oceanogr. 55(4), 1723-1732. https://doi.org/10.4319/lo.2010.55.4.1723

648 Venables, W.N., Ripley, B.D., 2002. Modern and Applied Statistics with S. Fourth edition. Springer, New
649 York. https://www.stats.ox.ac.uk/pub/MASS4

650 Venkiteswaran, J.J., Schiff, S.L., St. Louis, V.L., Matthews, C.J.D., Boudreau, N.M., Joyce, E.M., Beaty,
651 K.G., Bodaly, R.A., 2013. Processes affecting greenhouse gas production in experimental
652 borealreservoirs. Global Biogeochem. Cy. 27(2), 567-577.https://doi.org/10.1002/gbc.20046

653 Verdegem, M.C.J., Bosma, R.H., 2009.Water withdrawal forbrackish and inland aquaculture, and options
654 to producemore fish in ponds with present water use. Water Policy11 (Suppl 1), 52-68.

655 Wang, X.F., He, Y.X., Yuan, X.Z., Chen, H., Peng,C.H., Yue, J.S., Zhang, Q.Y., Diao, Y.B., Liu, S.S., 2017.
656 Greenhouse gases concentrations and fluxes from subtropical small reservoirs in relation with
657 watershed urbanization. Atmos. Environ. 154, 225-235.
658 https://doi.org/10.1016/j.atmosenv.2017.01.047

659 Wanninkhof, R., 1992. Relationship between wind speed and gas exchange over the ocean. J. Geophys.
660 Res. Oceans 97(C5), 7373-7382. https://doi.org/10.1029/92JC00188

661 Welti, N., Hayes, M., Lockington, D., 2017. Seasonal nitrous oxide and methane emissions across a
662 subtropical estuarine salinity gradient. Biogeochemistry 132,
663 55-69.https://doi.org/10.1007/s10533-016-0287-4

664 Wen, Z.D., Song, K.S.,, Zhao, Y., Jin, X.L., 2016. Carbon dioxide and methane supersaturation in lakes of
665 semi-humid/semi-arid region, Northeastern China. Atmos. Environ. 138: 65-73.
666 http://dx.doi.org/10.1016/j.atmosenv.2016.05.009

667 Wik, M., Varner, R.K., Anthony, K.W., MacIntyre, S., Bastviken, D., 2016. Climate-sensitive northern
668 lakes and ponds are critical components of methane release. Nat. Geosci. 9(2), 99.

669 World Meteorological Organization, 2017. WMO Greenhouse Gas Bulletin No.13 (October 2017).
670 https://library.wmo.int/opac/doc_num.php?explnum_id=3084.pdf.

671 Wu, S., Hu, Z.Q., Hu, T., Chen, J., Yu, K., Zou, J.W., Liu, S.W., 2018. Annual methane and nitrous oxide
672 emissions from rice paddies and inland fish aquaculture wetlands in southeast China. Atmos. Environ.
673 175, 135-144.https://doi.org/10.1016/j.atmosenv.2017.12.008

674 Wu, S., Li, S.Q., Zou, Z.H., Hu, T., Hu, Z.Q., Liu , S.W., Zou, J.W., 2019. High methane emissions largely
675 attributed to ebullitive fluxes from a subtropical river draining a rice paddy watershed in China.
676 Environ. Sci. Technol. 53, 349-3507. https://doi.org/10.1021/acs.est.8b05286

677 Xiao, S.B., Wang, C.H., Wilkinson, R.J., Liu,D.F., Zhang, C., Xu,W.N., Yang, Z.J., Wang, Y.C., Lei, D.,
678 2016. Theoretical model for diffusive greenhouse gas fluxes estimation across water-air interfaces
679 measured with the static floating chamber method. Atmos. Environ. 137, 45-52.
680 http://dx.doi.org/10.1016/j.atmosenv.2016.04.036

681 Xiao, Q.T., Zhang, M., Hu, Z.H., Gao, Y.Q., Hu, C., Liu, C., Liu, S.D., Zhang, Z., Zhao, J.Y., Xiao, W.,
682 Lee, X., 2017. Spatial variations of methane emission in a large shallow eutrophic lake in subtropical
683 climate. J. Geophys. Res. Biogeosci. 122 (7), 1597-1614. https://doi.org/10.1002/2017JG003805

684 Xiao, Q.T., Hu, Z.H., Fu, C.S., Bian, H., Lee, X.H., Chen, S.T., Shang, D.Y., 2019. Surface nitrous oxide
685 concentrations and fl uxes from water bodies of the agricultural watershed in Eastern China. Environ.
686 Pollut. 251, 185-192. https://doi.org/10.1016/j.envpol.2019.04.076

687 Xiao, W., Liu, S.D., Li, H.C., Xiao, Q., Wang, W., Hu, Z.H., Hu, C., Gao, Y.Q., Shen, J., Zhao, X.Y., Zhang,
688 M., Lee, X.H., 2014. A flux-gradient system for simultaneous measurement of the CH_4, CO_2, and H_2O
689 fluxes at a lake-air interface. Environ. Sci. Technol. 48, 14490-14498.
690 https://doi.org/10.1021/es5033713

691 Xing, Y., Xie, P., Yang, H., Ni, L., Wang, Y., Tang, W., 2004. Diel variation of methane fluxes in summer in
692 a eutrophic subtropical lake in China. J. Freshwa. Ecol. 19, 639-644.
693 https://doi.org/10.1080/02705060.2004.9664745

694 Yan, F., Sillanpää, M., Kang, S., Aho, K. S.,Qu, B., Wei, D., et al. (2018). Lakes on theTibetan Plateau as
695 conduits ofgreenhouse gases to the atmosphere. J. Geophys. Res.-Biogeo. 123, 2091-2103.
696 https://doi.org/10.1029/2017JG004379

697 Yang, H., Xie, P., Ni, L.Y., Flower, R.J., 2011. Underestimation of CH_4 emission from freshwater lakes in
698 China. Environ. Sci. Technol.45(10), 4203-4204. https://doi.org/10.1021/es2010336

699 Yang, P., Bastviken, D., Jin, B.S., Mou, X.J., Tong, C., 2017a. Effects of coastal marsh conversion to
700 shrimp aquaculture ponds on CH_4 and N_2O emissions. Estuar. Coast. Shelf S. 199,
701 125-131.https://doi.org/10.1016/j.ecss.2017.09.023.

702 Yang, P., He, Q.H., Huang, J.F., Tong, C., 2015. Fluxes of greenhouse gases at two different aquaculture
703 ponds in the coastal zone of southeastern China. Atmos. Environ. 115,
704 269-277.https://doi.org/10.1016/j.atmosenv.2015.05.067

Yang, P., Lai, D.Y.F., Jin, B.S., Bastviken, D., Tan, L.S., Tong, C., 2017b. Dynamics of dissolved nutrients in the aquaculture shrimp ponds of the Min River estuary, China: Concentrations, fluxes and environmental loads. Sci. Total Environ. 603-604, 256-267.https://doi.org/10.1016/j.scitotenv.2017.06.074

Yang, P., Zhang, Y., Yang, H., Zhang, Y. F., Xu, J., Tan, L.S., Tong, C., Lai, D.Y.F., 2019. Large fine-scale spatiotemporal variations of CH_4 diffusive fluxes from shrimp aquaculture ponds affected by organic matter supply and aeration in Southeast China. J. Geophys. Res.-Biogeo. 124, 1290-1307. https://doi.org/10.1029/2019JG005025

Yang, P., Zhang, Y., Bastviken, D., Lai, D.Y.F., Yang, H., Zhang, Y.F., Guo, Q.Q., Tan, L.S., Tong, C., 2020. Large increase in diffusive greenhouse gas fluxes from subtropical shallow aquaculture ponds during the passage of typhoons. J. Hydrol. 583, 124643. https://doi.org/10.1016/j.jhydrol.2020.124643

Yuan, J. J., Xiang, J., Liu, D. Y., Kang, H., He, T. H., Kim, S., et al. (2019). Rapid growth in greenhouse gas emissions from the adoption of industrial-scale aquaculture. Nat.Clim. Chang. 9(4), 318-322. https://doi.org/10.1038/s41558-019-0425-9

Zappa, C.J., McGillis, W.R., Raymond, P.A., Edson, J.B., Hintsa, E.J., Zemmelink, H.J., Dacey, J.W.H., Ho, D.T., 2007. Environmental turbulent mixing controls on air-water gas exchange in marine and aquatic systems. Geophys. Res. Lett. 34(10), L10601. https://doi.org/10.1029/2006GL028790

Zhang, Y.F., Yang, P., Yang, H., Tan, L.S., Guo, Q.Q., Zhao, G.H., Li, L., Gao, Y.C., Tong, C., 2019. Plot-scale spatiotemporal variations of CO_2 concentration and flux across water-air interfaces at aquaculture shrimp ponds in a subtropical estuary. Environ. Sci. Pollut. R. 26, 5623-5637. https://doi.org/10.1007/s11356-018-3929-3

Zhao, J.Y., Zhang, M., Xiao, W., Wang, W., Zhang, Z., Yu, Z., Xiao,Q.T., Cao, Z.D., Xu, J.Z., Zhang, X.F., Liu, S.D., Lee, X.H., 2019. An evaluation of the flux-gradient and the eddy covariance method to measure CH_4, CO_2, and H_2O fluxes from small ponds. Agr. Forest Meteorol. 275, 255-264. https://doi.org/10.1016/j.agrformet.2019.05.032

Zhao, Y., Sherman, B., Ford, P., Demarty, M., DelSontro, T., Harby,A., Tremblay, A., Øverjordet, I.B., Zhao, X.F., Hansen, B.H., Wu, B.F., 2015. A comparison of methods for the measurement of CO_2 and

CH_4 emissions from surface water reservoirs: Results from an international workshop held at Three Gorges Dam, June 2012. Limnol. Oceanogr.: Methods 13, 15-29. https://doi.org/10.1002/lom3.10003

Zhao, Y., Wu, B. F., Zeng, Y., 2013. Spatial and temporal patterns of greenhouse gas emissions from Three Gorges Reservoir of China. Biogeosciences 10, 1219-1230. https://doi.org/10.5194/bg-10-1219-2013

Zhu, D., Wu, Y., Chen, H., He, Y. X., Wu, N., 2016. Intense methane ebullition from open water area of a shallow peatland lake on the eastern Tibetan Plateau. Sci. Total Environ. 542, 57-64. https://doi.org/10.1016/j.scitotenv.2015.10.087

Table 1

Summary of the *TBL* and *FCs* methods applied to measure CH_4 diffusive fluxes from the aquaculture ponds in Min River Estuary during the aquaculture period.

	***TBL* methods**						***FCs* method**
	TBL_{LM86}	TBL_{W92a}	TBL_{RC01}	TBL_{CL98}	TBL_{W92b}	TBL_{CW03}	
Minimum (μmol m^{-2} h^{-1})	0.6	1.3	5.6	1.9	1.9	1.3	1.3
Maximum (μmol m^{-2} h^{-1})	108.8	650.0	1079.4	527.5	454.4	428.8	476.3
Average (μmol m^{-2} h^{-1})	19.4	103.1	215.6	115.0	78.1	75.0	71.9
Standard deviation	23.1	130.6	236.3	122.5	91.3	86.9	88.8
Coefficient of variation	1.18	1.27	1.09	1.06	1.16	1.15	1.24

Table 2

Pearson correlation coefficients for dissolved CH_4 concentration, CH_4 diffusive fluxes and environmental variables from the aquaculture ponds in Min River Estuary during the aquaculture period[a]. Bold numbers denote correlation coefficients for significant relationships.

Environmental variables	Dissolved CH_4 concentration	CH_4 diffusive fluxes
Meteorological parameters		
Air temperature	**0.214***	**0.203***
Wind speed (W_S)	NS	**0.281***
Atmospheric pressure	NS	NS
Water parameters		
Water temperature	NS	NS
Dissolved oxygen (DO)	NS	NS
TOC concentration	**0.312****	**0.296****
N-NO_3^- concentration	**-0.401****	**-0.392****
Electrical conductivity (EC)	**-0.361****	**-0.185***

[a] The symbols * and ** indicate significant correlations at the 0.05 and 0.01 levels, respectively. n = 135 for environmental variables and CH_4 diffusive fluxes from the aquaculture ponds. CH_4 diffusive fluxes were directly measured using floating chambers method.

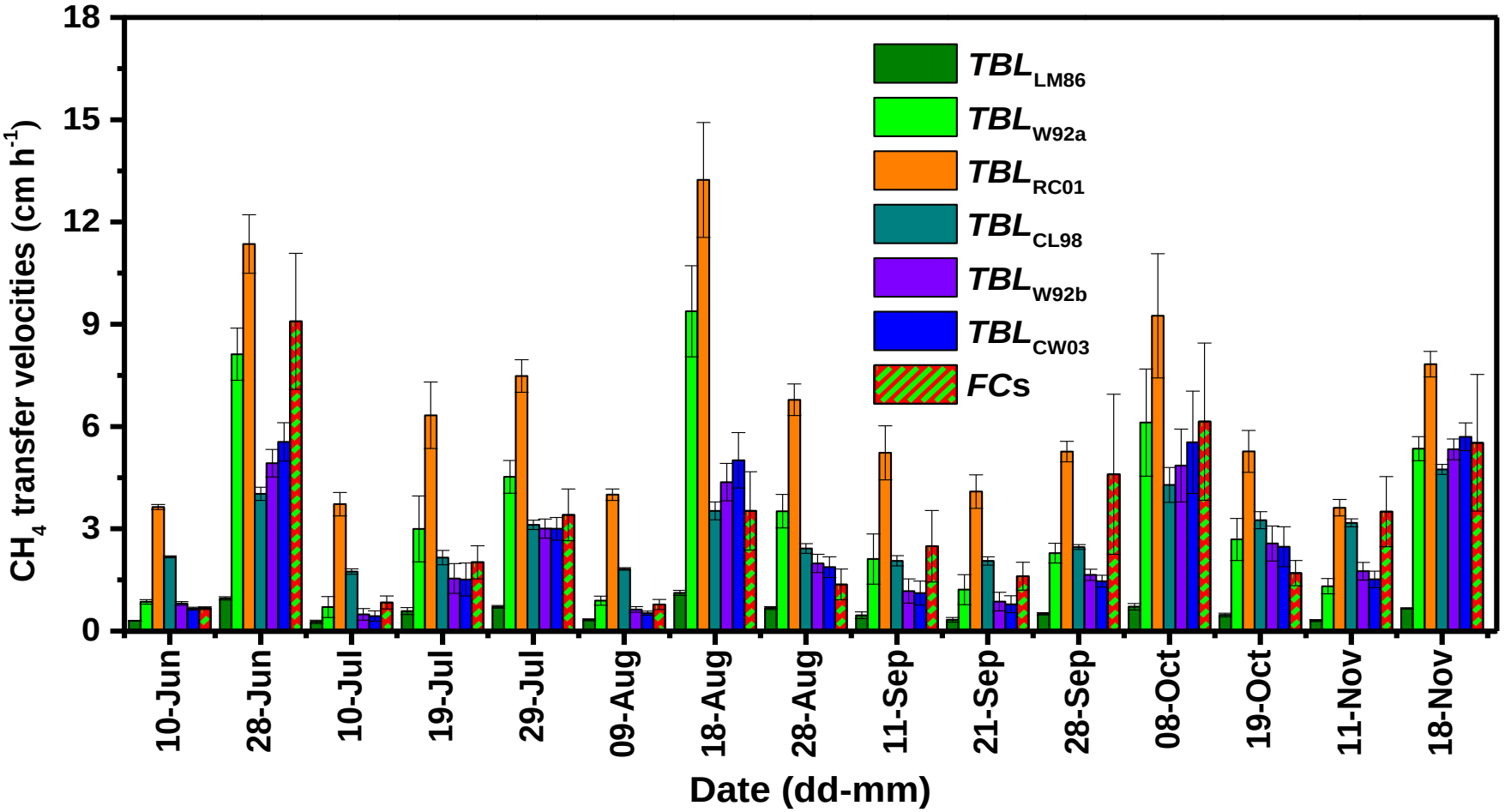

748

749 **Figure 1.** Temporal variation in CH_4 transfer velocities from the aquaculture ponds during the aquaculture period in the Min River

750 Estuary. Values represent the means of nine replicates samples, while the vertical lines indicate standard errors .

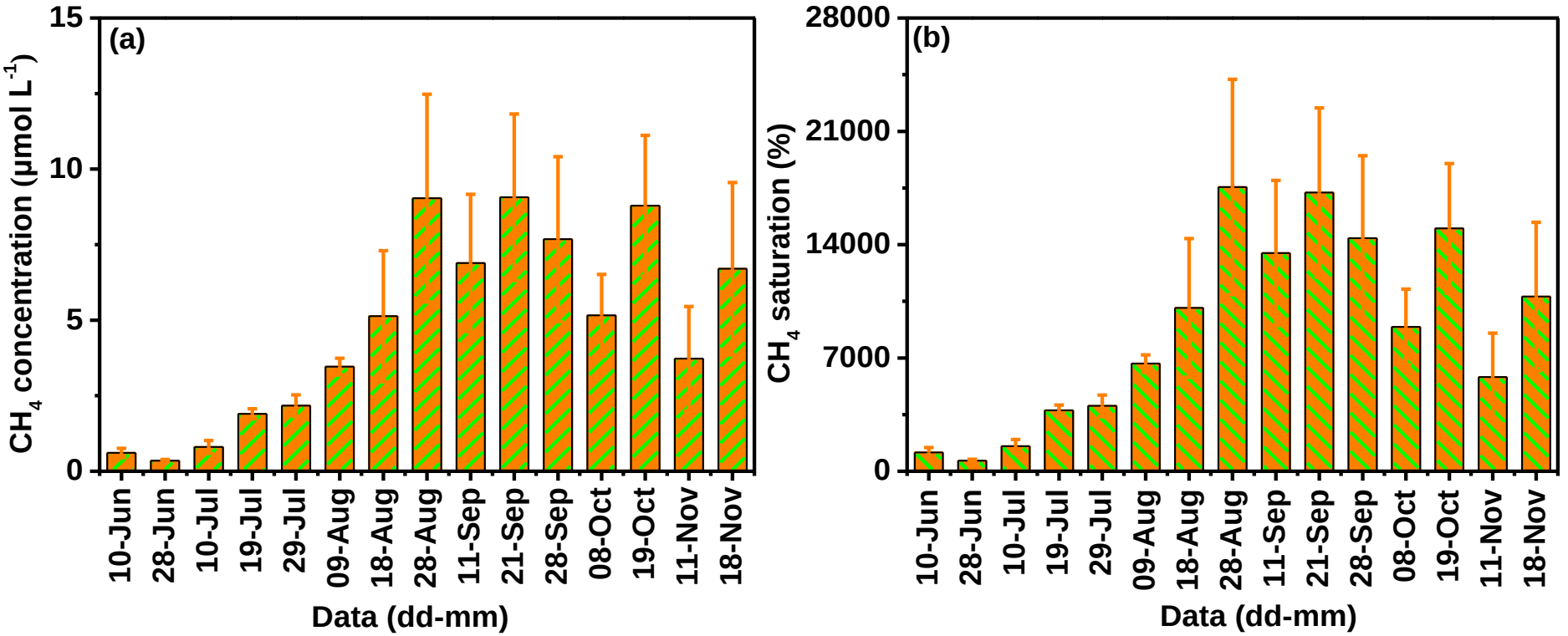

Figure 2. Temporal variation in (a) CH_4 concentration and (b) CH_4 saturation in the surface water (20 cm depth) of the aquaculture ponds in the Min River Estuary during the aquaculture period. Values represent the means of nine replicates samples, while the vertical lines indicate standard errors.

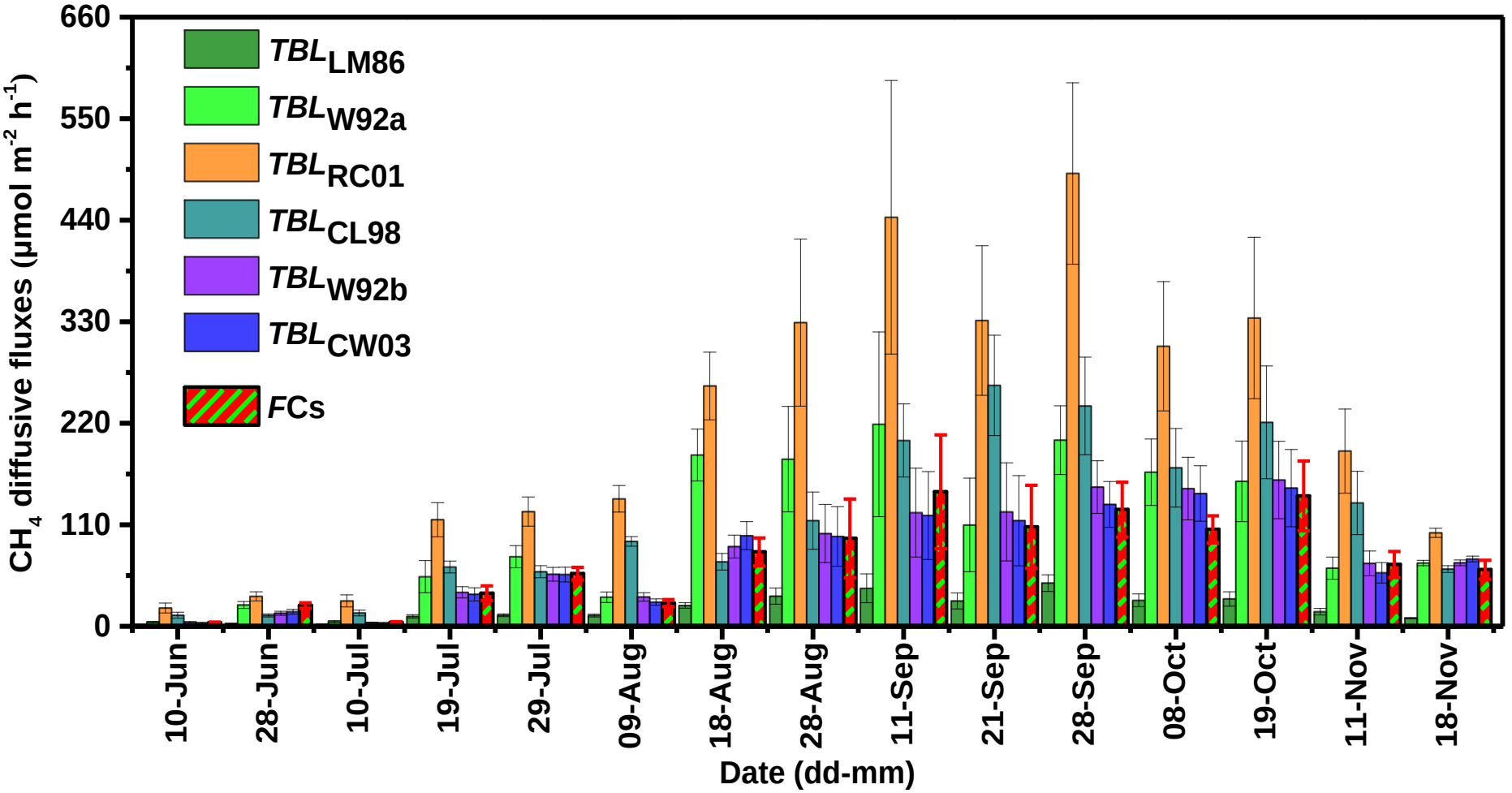

Figure 3. Temporal variation in CH_4 diffusive fluxes measured with the floating chamber method and the gas transfer velocity model methods during the aquaculture period from the aquaculture ponds in the Min River Estuary. Values represent the means of nine replicates samples, while the vertical lines indicate standard errors.

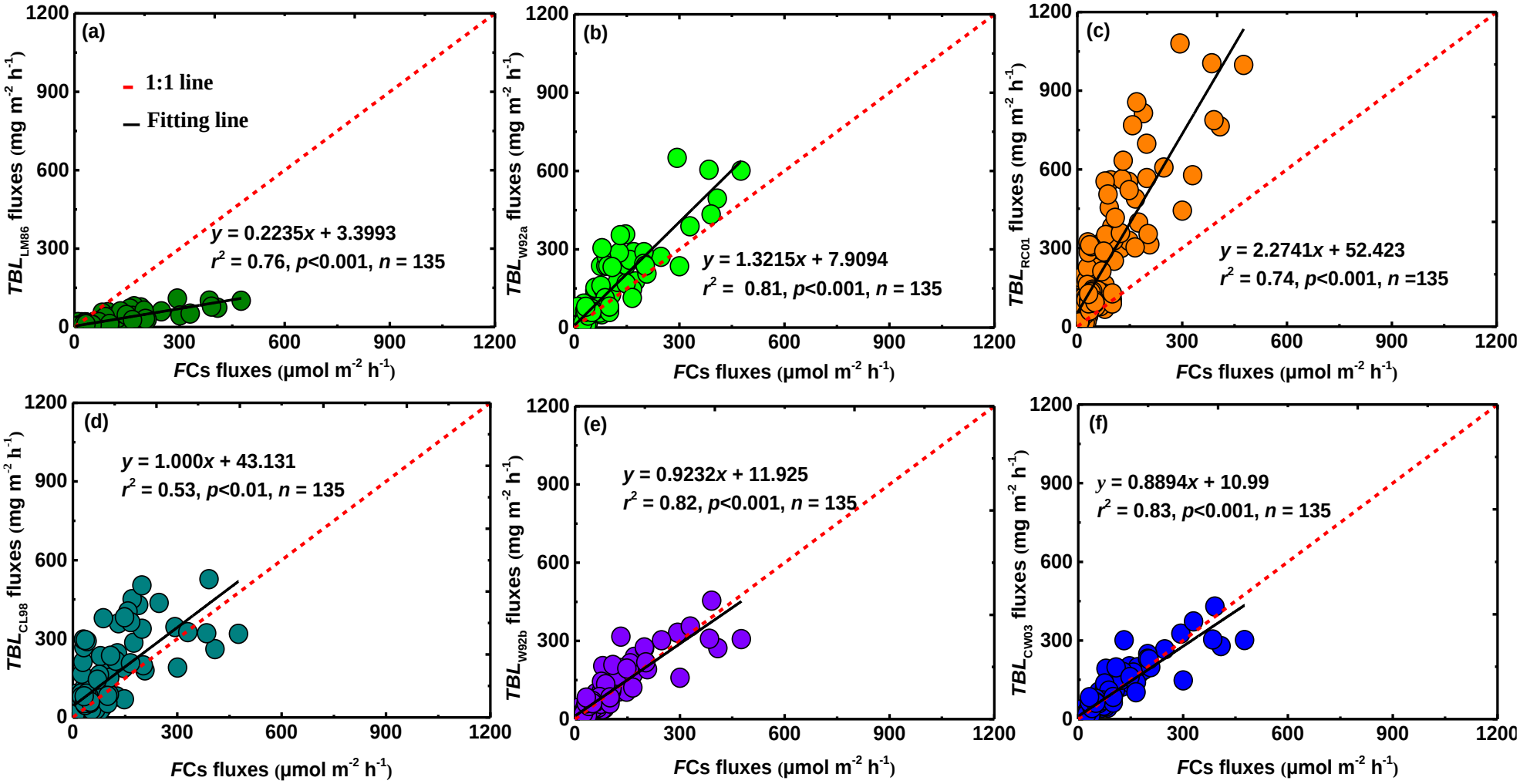

759

760 **Figure 4.** Comparison of CH_4 diffusive flux measured by using the *FCs* method and *TBL* models. Regression equation, linear correlation (r^2) and

761 significance (p) are also shown. Parameter bounds on the regression coefficients are 95% confidence intervals.

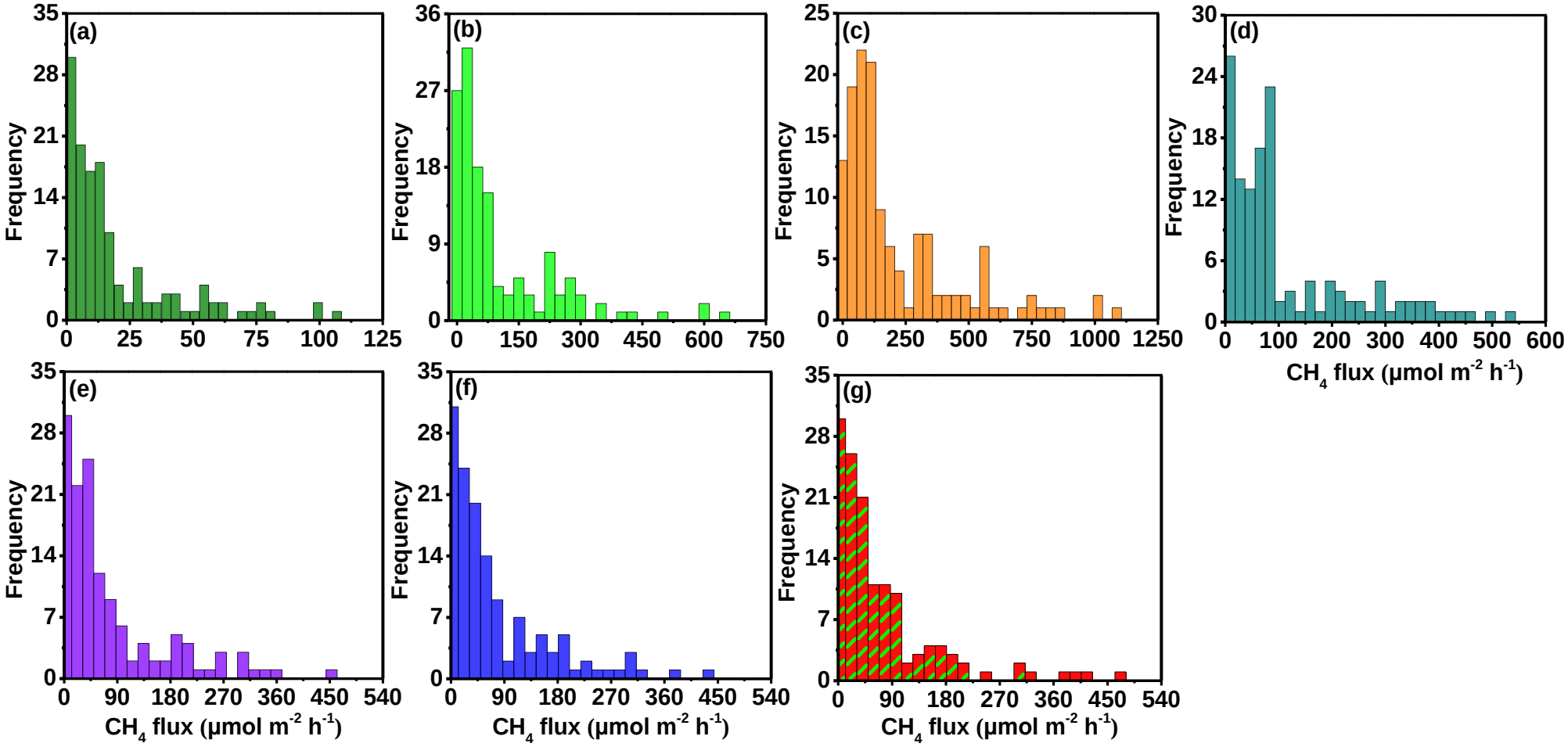

762

763 **Figure 5.** Frequency distribution of CH_4 diffusive fluxes from (a) TBL_{LM86}, (b) TBL_{W92a}, (c) TBL_{RC01}, (d) TBL_{CL98}, (e) TBL_{W92b}, (f) $TBL_{CW03,}$ and

764 (g) FCs measurements at the aquaculture ponds in the Min River Estuary during the aquaculture period.

765